

# Optical Interferometers with Reduced Sensitivity to Thermal Noise

H. J. Kimble<sup>†</sup>, Benjamin L. Lev<sup>‡</sup>, and Jun Ye

*JILA, National Institute of Standards and Technology and University of Colorado, Boulder, CO 80309-0440*  
(Dated: November 19, 2021)

A fundamental limit to the sensitivity of optical interferometry is thermal noise that drives fluctuations in the positions of the surfaces of the interferometer's mirrors, and thereby in the phase of the intracavity field. Schemes for reducing this thermally driven phase noise are presented in which phase shifts from concomitant strains at the surface and in the bulk of the substrate compensate the phase shift due to the displacement of the surface. Although the position of the physical surface fluctuates, the optical phase upon reflection can have reduced sensitivity to this motion.

Thermal noise presents a fundamental limit to measurement sensitivity in diverse areas of science and technology [1]. One important setting is that of optical interferometry in which otherwise stable structures experience small, thermally driven fluctuations in their dimensions in applications ranging from frequency metrology [2, 3, 4], to gravitational wave detection [5, 6], to the realization of quantum behavior for macroscopic objects [7].

The dominant limitation to length stability for some interferometers originates from thermally driven displacement noise for the reflective surfaces of the mirror substrates, and not from the external, support structure [3, 4, 6]. The fluctuations of the mirror surfaces are of fundamental origin and arise from dissipation in the elasticity of the substrate as demanded by the Fluctuation-Dissipation Theorem (FDT) [8, 9, 10].

Beyond displacements driven by thermal noise in the substrate itself [11, 12, 13, 14, 15, 16], diverse other sources of mechanical noise have been identified in recent years, including noise from frictional losses in the materials that form the mirror coating [14, 17], thermoelastic-damping in the substrate and coating [16, 18, 19], and thermo-refractive noise [20]. Measurements of phase noise in rigid [2, 3, 4] and suspended interferometers [21, 22, 23] have confirmed many characteristics of individual noise sources.

Various avenues have been followed for reducing thermal noise in optical interferometers, the most significant being lowering mechanical losses for the substrate [1, 24] and, more recently, the coating [23, 25]. New designs for advanced interferometers include the use of a corner reflector [26] or a short Fabry-Perot (FP) cavity [27] to replace the usual single surface of a mirror.

In this Letter, we propose a new strategy for reducing thermally driven phase noise in optical interferometers. Fundamental to our proposal is the observation that stochastic displacements  $\delta u_z$  perpendicular to the mirror's surface are necessarily accompanied by correlated strains in the underlying materials of the mirror coating and substrate. In a conventional setting, the phase shift  $\delta\beta$  due to these strains in the coating and substrate are small compared to the phase shift  $\delta\theta$  from the surface motion  $\delta u_z$ . However, by suitable design, it should be possible to achieve a total phase shift  $\delta\Phi = \delta\beta + \delta\theta \simeq 0$

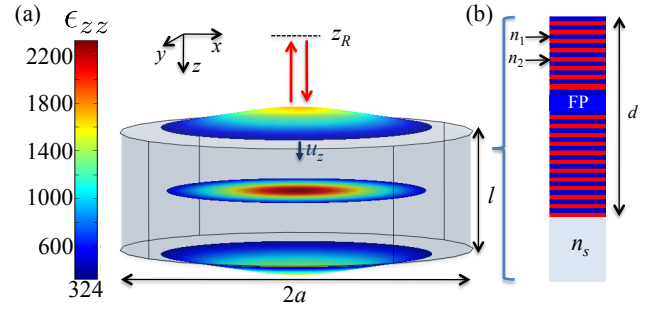


FIG. 1: (color online) (a) The undistorted shape of a sapphire substrate of radius  $a = 1.5$  mm and thickness  $l = 1$  mm is depicted by the shaded region and wire frame. Axial displacements  $u_z(x, y, z)$  and strains  $\epsilon_{zz}(x, y, z)$  are shown across planes at  $z = 0, l/2, l$  (top to bottom) for the eigenmode  $\xi_0(\mathbf{r})$  with eigenfrequency  $\omega_0/2\pi = 2.22$  MHz. Plotted are contours for  $u_z(x, y, z)$  on which  $\epsilon_{zz}(x, y, z)$  is color coded at a time of maximum axial extension, where  $u_z(x, y, z) = 0$  absent excitation. The phase for propagation from  $z = z_R$  to the substrate and back is modified by surface motion  $u_z$  at  $z = 0$ . (b) Coating stack for a high reflectivity mirror with embedded FP cavity for high strain sensitivity.

for the reflected field. That is, although the physical surface of the mirror is subject to random displacements  $\delta u_z$ ,  $\delta\Phi$  can be insensitive to these displacements with  $\delta\theta$  dynamically compensated by  $\delta\beta$  from the coating and substrate. Although our current analysis is for “Brownian noise” of the substrate, our methodology should be applicable to thermoelastic and coating noise as well.

As a first example, consider thermal noise for an eigenmode of a cylindrical mirror with mechanical resonance frequency  $\omega_0$ . For frequencies  $\omega \simeq \omega_0$  and quality factor  $Q_0 \gg 1$ , microscopic thermal noise excites the entire “shape” of the relevant eigenmode  $\xi_0(\mathbf{r})$ , with a single, overall amplitude set by equipartition of energy [11, 12]. The amplitude  $\delta u_z$  and accompanying strain  $\epsilon_{zz}$  for thermally driven motion perpendicular to the mirror surface at  $z = 0$  are then determined directly from  $\xi_0(\mathbf{r})$ .

Figure 1(a) illustrates a particular axisymmetric eigenmode  $\xi_0(\mathbf{r})$  for a sapphire substrate of mass  $M$  as determined from a numerical finite-element analysis. For this mode, the end faces at  $z = 0, l$  oscillate in oppo-

sition about the plane at  $z = l/2$  with frequency  $\omega_0$ . In thermal equilibrium at temperature  $T$ ,  $\delta u_z$  at the central points  $x, y = 0$  on the end faces has amplitude  $\langle \delta u_z^2 \rangle_{\omega_0} \simeq k_B T / M_0 \omega_0^2$ , where  $M_0$  is the effective mass [12], which for the mode shown is  $M_0 = 2.7M$ . Significant to our current investigation is the axial strain per unit displacement,  $\zeta \equiv \epsilon_{zz}/u_z$ , where  $\zeta \simeq -1600/\text{m}$  at  $x, y, z = 0$  for the parameters in Fig. 1(a) (i.e., expansion at  $z = 0$  with  $u_z < 0$  generates strain  $\epsilon_{zz} > 0$ ).

As depicted in Fig. 1, we next address the question of the phase shift for light reflected from the fluctuating surface of the substrate at  $z = 0$ . Following Levin [14], we introduce the displacement  $q(z)$  weighted by the normalized light intensity  $\psi(r)$  over a plane at depth  $z \geq 0$ , namely  $q(z) = \int dx dy \delta u_z(r, z) \psi(r)$ , where  $\psi(r) = (2/\pi w_0^2) \exp(-2r^2/w_0^2)$  with  $r = \sqrt{x^2 + y^2}$ . The incident field with vacuum wavevector  $k$  experiences a phase change  $\delta\theta = -2kq(z=0) \equiv -2kq_0$  for the reflected field due to the “piston” motion of the surface.

In addition to  $\delta\theta$ , strain that accompanies surface motion modifies the optical coating and thereby leads to a phase shift  $\delta\beta$ , with  $\delta\beta$  expressed relative to the front surface of the coating. The overall phase shift for the reflected field is then  $\delta\Phi = \delta\theta + \delta\beta$ , with  $|\delta\beta| \ll |\delta\theta|$  for typical optical coatings. We now present new designs for the coating to achieve  $\delta\Phi = \delta\theta + \delta\beta \simeq \delta\theta/Q_0$ .

The coating structure shown in Fig. 1(b) has an embedded resonant layer that functions as a FP cavity and gives rise to a rapid phase variation near the cavity resonance [28]. Explicitly, the coating structure is specified as  $n_0(\eta_1\eta_2)^l\eta_1(j \times \eta_{FP})(\eta_1\eta_2)^{p-l}n_s$ . Starting from the vacuum side  $n_0 = 1$ , there are  $l$  double-layers  $(\eta_1\eta_2)^l$  with  $\eta_{1,2} = \pi/2$  at the reference wavevector  $k_0$ , followed by an  $n_1$  layer with  $\eta_1 = \pi/2$  at  $k_0$ , then the FP  $n_1$  layer with single-pass phase shift  $j \times \eta_{FP}$  at  $k_0$ , followed by the terminating  $p-l$  double layers, and lastly the substrate with index  $n_s$ . We restrict attention to the case of a “thin” coating for which the total coating thickness  $d \ll a, w_0$  and further assume that the axial strain in the coating  $\epsilon_{zz}^c$  is the same as that in the substrate  $\epsilon_{zz}$ . These assumptions simplify the discussion of the essential aspects of our scheme for noise compensation; see Refs. [23, 25] for detailed treatments of multilayer coatings. A discussion of thermal noise from the coating itself is deferred to our concluding remarks.

Results for two particular coatings are given in Fig. 2 for  $w_0 \ll a$ . For definiteness, we assume a coating stack made from layers of  $\text{SiO}_2$  with index  $n_1 = 1.45$  and  $\text{Ta}_2\text{O}_5$  with  $n_2 = 2.03$ . Parts (a, b) are for displacement-induced strain  $\zeta = -1600/\text{m}$ , as appropriate to  $\xi_0(\mathbf{r})$  in Fig. 1(a). The coating structure is  $[p = 33, l = 8]$  with three curves drawn for mode orders  $j = 1, 4, 16$  with  $\eta_{FP} = \pi$ . In (a), increased length for the resonant structure leads to greater strain sensitivity, with  $|\delta\beta|$  becoming larger relative to  $|\delta\theta|$ . For  $j = 16$  there arise “magic” wavevectors  $k_{\pm}$  for which  $\delta\Phi(k_{\pm}) = 0$ , with then the piston phase shift  $\delta\theta$  from fluctuations of the surface dynamically compensated by the strain-induced phase shift

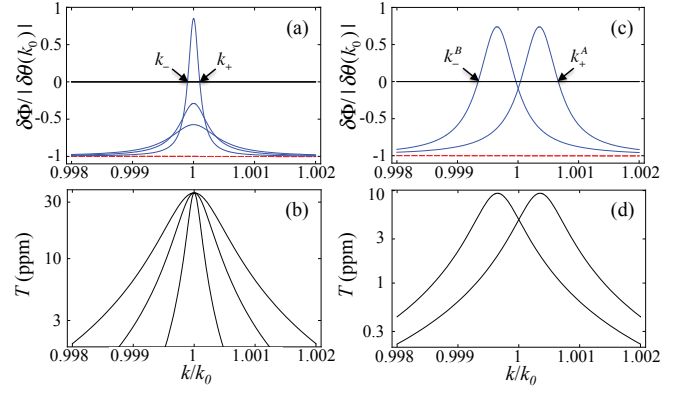


FIG. 2: Phase shift  $\delta\Phi(k)$  and transmission coefficient  $T(k)$  for two different coating designs illustrated in Fig. 1(b) and specified in the text. (a, b) The case  $\zeta = -1600/\text{m}$  for increasing phase  $j\eta_{FP}$  of the internal resonant structure. (a) Total phase  $\delta\Phi(k)$  with “magic” wavevectors  $k_{\pm}$  and (b) associated transmission coefficient  $T(k)$  for  $j = 1, 4, 16$  from widest to narrowest curves. (c, d)  $\delta\Phi(k)$  and  $T(k)$  for the case  $\zeta = -5000/\text{m}$  for two coatings with slightly different internal resonances  $\eta_{FP}^{(A,B)}$  with distinct values  $k_{\pm}^B, k_{\pm}^A$  for nulling noise from mirrors  $B, A$ . In all cases,  $\delta\Phi(k)/|\delta\theta(k_0)|$  is plotted for  $q_0 > 0$ , with  $\delta\theta(k)$  given by the dashed lines in (a, c).

$\delta\beta$  from the coating. At these “magic wavelengths,” the phase of the reflected optical field becomes insensitive to the thermal motion of the surface of the substrate.

Figures 2(c,d) investigate the possibility that thermal noise of individual mirrors of an interferometer could be measured *in situ*. The coating for each of two mirrors  $A, B$  is specified by  $[p = 33, l = 7, j = 8]$ . The thicknesses of the FP layers in the  $A, B$  coatings have been adjusted to give  $\eta_{FP}^{(A,B)} = (0.9995, 1.0005) \times \pi$  at  $k_0$  for the two traces shown. For operation at the lower (upper) value  $k_{\pm}^B(k_{\pm}^A)$  noise from mirror  $B(A)$  would be nulled while that from mirror  $A(B)$  would be  $\sim 80\%$  of the full piston phase, so that the noise arising from mirrors  $A, B$  could be individually measured. For operation at the central value  $k/k_0 = 1$ , thermal noise from both mirrors  $A, B$  would be suppressed. Panel (d) gives the transmission coefficient  $T(k) = 1 - R(k)$  for the two coatings, where  $T(k_{\pm}^B, k_{\pm}^A)$  is consistent with high-finesse measurements. Not shown in Fig. 2 are FP resonances away from  $k \approx k_0$ , which can also be employed to suppress thermal noise.

Because the surface strain  $|\zeta|$  decreases with increasing size of the substrate, compensation of the piston phase  $\delta\theta$  with increasing  $a, w_0$  requires greater departures from standard coating designs, material specifications, and fabrication procedures. Moreover, not all eigenmodes of oscillation have the proper parity (i.e.,  $\zeta < 0$ ) for compensation by way of the coating designs in Fig. 2.

A second, more challenging example is thermal noise at frequencies  $\omega$  well below the lowest resonance of the mirror substrate. In this quasi-static regime, we must understand the correlation between thermal displacements at depth  $z$  and fluctuations of the surface arising from

many modes [12]. The foundation for our analysis is the FDT [8, 9] as applied by Levin to this setting [14].

We consider a substrate in the form of an infinite half space with boundary at  $z = 0$  and extending to  $z \geq 0$ . Equation (9) in Mindlin [29] provides the Green's function required to deduce the admittance for application of the FDT from Eq. (6.8) of Ref. [9]. Following the techniques in [16], we find the spectral correlation for beam-averaged axial displacements  $\tilde{q}(z)$  at depths  $z_1, z_2$  to be

$$\langle \tilde{q}(z_2) \tilde{q}(z_1) \rangle_\omega = \langle \tilde{q}_0 \tilde{q}_0 \rangle_\omega N(z_2, z_1), \quad (1)$$

where  $\tilde{q}(z_i) \equiv \tilde{q}(z_i, \omega)$  is the Fourier transform of  $q(z_i, t)$ .  $\langle \tilde{q}_0 \tilde{q}_0 \rangle_\omega = 2k_B T (1 - \sigma^2) \phi_s / \pi^{3/2} w_0 E \omega$  is the standard result for thermally driven surface displacements, with  $E, \sigma$  the Young's modulus and Poisson ratio, respectively, and  $\phi_s$  the (possibly frequency dependent) loss angle for the substrate. The function  $N(z_2, z_1)$  determines the mechanical admittance and is given by

$$N(z_2, z_1) = \frac{w_0}{8\sqrt{\pi}(1 - \sigma)^2} \int_0^\infty dk e^{-k^2 w_0^2/4} f(z_2, z_1; k),$$

where

$$f(z_2, z_1; k) = e^{-k|z_-|} [3 - 4\sigma + k|z_-|] + e^{-kz_+} [5 - 12\sigma + 8\sigma^2 + k(3 - 4\sigma)z_+ + 2k^2 z_1 z_2], \quad (2)$$

with  $z_\pm = z_1 \pm z_2$  and  $N(z, z)$  plotted in Fig. 3(a). Note that  $N(0, 0) = 1$ ,  $N(z_1, z_2) = N(z_2, z_1)$  [10], and that the admittance derived from  $N(z, 0)$  agrees with that from previous work [14, 16, 17].

Equation (1) enables us to determine spectral correlations between thermally driven axial displacements at depths  $z_1, z_2$  characterized by [30]

$$C(z_1, z_2) = \frac{\langle \tilde{q}(z_1) \tilde{q}(z_2) \rangle}{\langle \tilde{q}(z_1) \tilde{q}(z_1) \rangle^{1/2} \langle \tilde{q}(z_2) \tilde{q}(z_2) \rangle^{1/2}}, \quad (3)$$

where  $C(z, z) = 1$  and  $|C(z_1, z_2)| \leq 1$ . From Fig. 3(a), we see that thermal fluctuations of  $\tilde{q}(z)$  correlate over length scales set by  $w_0$ , albeit with decreasing amplitude  $\langle \tilde{q}(z) \tilde{q}(z) \rangle \propto N(z, z)$  away from the surface.

Figure 3(b) investigates correlation between displacement  $\tilde{q}(z_1)$  at  $z_1$  and axial strain at depth  $z_2$  by way of the function  $Q(z_1; z_2, \Delta z_2) = \varepsilon_z^{\text{coh}}(z_1, z_2) / \varepsilon_z^{\text{tot}}(z_2, \Delta z_2)$ , with  $|Q| \leq 1$ .  $Q(z_1; z_2, \Delta z_2)$  expresses the ratio of coherent to total strain at  $z_2$  within a small slice  $\Delta z_2$ , where  $\varepsilon_z^{\text{coh}}(z_1, z_2) \equiv \langle \tilde{q}(z_1) [\tilde{q}(z_2 + \Delta z_2) - \tilde{q}(z_2)] / \Delta z_2 \rangle / \langle \tilde{q}(z_1)^2 \rangle^{1/2}$  is the strain at  $z_2$  correlated with the displacement  $\tilde{q}(z_1)$  at  $z_1$ , while  $\varepsilon_z^{\text{tot}}(z_2, \Delta z_2) \equiv \langle [\tilde{q}(z_2 + \Delta z_2) - \tilde{q}(z_2)]^2 \rangle^{1/2} / \Delta z_2$  is the total strain at  $z_2$ .

In Fig. 3(b), the spatial scale for correlation of displacement and strain is again set by  $w_0$ , but now with magnitude reduced by  $\sqrt{\Delta z_2 / w_0}$ . This scaling of  $Q$  can be understood from the fact that the rms strain diverges as  $1/\sqrt{V}$  for thermal fluctuations in a volume  $V$  [31], which motivates our use of finite differences to characterize strain. Near the surface at  $z = 0$

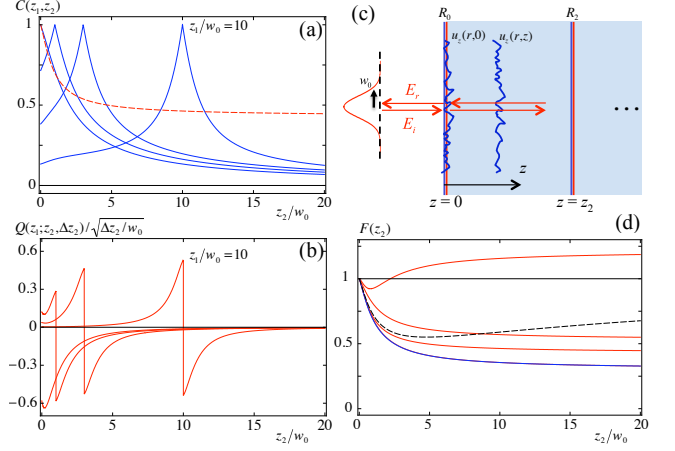


FIG. 3: (a) Correlation of thermally driven axial displacements  $C(z_1, z_2)$  and (b) displacement-strain correlation  $Q(z_1; z_2, \Delta z_2) / \sqrt{\Delta z_2 / w_0}$  versus  $z_2 / w_0$  for  $z_1 / w_0 = 0, 1, 3, 10$ , with  $\Delta z_2 / w_0 = 10^{-3}$  in (b). The dashed trace in (a) is  $N(z_2, z_2)$ . (c) Illustration of the mirror geometry discussed in the text. (d) Spectral density of phase fluctuations  $F(z_2)$  for the reflected field  $\mathbf{E}_r$  for the configuration in (c) for an  $\text{SiO}_2$  substrate. From top to bottom, the curves are for  $\alpha = 1.5, 0.3, 1.0, 0.7$  with the blue trace for  $\alpha = \alpha_{\min}$  overlaying the curve for  $\alpha = 0.7$ . The dashed curve is from a simple model that incorporates incoherent contributions from transverse strains to  $\delta\beta$ . All curves are for  $\sigma = 0.2$ .

with  $\Delta z / w_0 \ll 1$ , we find from Eq. (1) that  $\varepsilon_z^{\text{tot}}(z \simeq 0, \Delta z) \sim [\langle \tilde{q}_0 \tilde{q}_0 \rangle / (\Delta z w_0)]^{1/2}$ , where the relevant volume is  $V \sim \pi w_0^2 \Delta z$ . On the other hand, the coherent strain  $\varepsilon_z^{\text{coh}} \equiv \varepsilon_z^{\text{coh}}(0, 0) \sim -\langle \tilde{q}_0 \tilde{q}_0 \rangle^{1/2} / w_0$ , so that  $|\varepsilon_z^{\text{coh}} / \varepsilon_z^{\text{tot}}|$  scales as  $\sqrt{\Delta z / w_0} \ll 1$  near  $z = 0$ .

Simply stated, thermally driven surface motion  $\tilde{q}_0$  arises from strains within the substrate over distances  $z \gtrsim w_0$ . Hence, our previous strategy with a thin optical coating of thickness  $\Delta z = d \ll w_0$  employed as a surface-strain sensor for a single eigenmode will compensate only a small fraction of the phase shift  $\delta\theta = -2k\tilde{q}_0$  from the surface motion in the quasi-static regime. Instead, we must find a geometry for which  $\delta\beta$  has contributions over  $z \gtrsim w_0$  sufficient to compensate  $\delta\theta$ .

An initial mirror geometry that attempts to achieve such compensation is illustrated in Fig. 3(c). A thin dielectric coating with reflectivity  $R_0$  is deposited on the surface of the substrate at  $z = 0$ , and a second reflecting surface is embedded at  $z = z_2 \ll nk w_0^2 / 2$  with reflectivity  $R_2 \rightarrow 1$ . In the static case, an incident field  $\mathbf{E}_i$  linearly polarized along  $x$  is reflected from this two-mirror geometry to give a field  $\mathbf{E}_r$  with  $\mathbf{E}_r / \mathbf{E}_i = A e^{i\Gamma(\varphi)}$ , where  $\varphi$  is the roundtrip, internal phase, and  $A = 1$  for  $R_2 = 1$ . Thermally driven fluctuations lead to a phase shift  $\delta\Phi$  for  $\mathbf{E}_r$ ,  $\delta\Phi = -2k [\tilde{q}_0 + \alpha(k) (\tilde{q}(z_2) - \tilde{q}_0)]$ , where the piston phase is  $\delta\theta = -2k\tilde{q}_0$  and the interferometer phase is  $\delta\beta = -2k\alpha(k) (\tilde{q}(z_2) - \tilde{q}_0)$ .  $\alpha(k)$  expresses the sensitivity of the composite cavity  $R_0, R_2$  to strain driven

changes in both length and index around  $\varphi_0$ , with

$$\alpha(k) = n_s \left( 1 - \frac{n_s^2 p_{12}}{2} \right) \left| \frac{d\Gamma(\varphi_0)}{d\varphi} \right|, \quad (4)$$

where  $p_{12}$  is an element of the strain-optic tensor  $p_{ij}$  for an assumed isotropic material. In Eq. 4, we neglect contributions from fluctuating strains transverse to the propagation direction  $z$ , which are considered below.

The expressions for  $\delta\Phi$  and  $\alpha(k)$  lead to the spectral density  $\langle(\delta\Phi)^2\rangle$  of phase fluctuations for the reflected field  $\mathbf{E}_r$ , namely  $\langle(\delta\Phi)^2\rangle = \langle(\delta\theta)^2\rangle[(1-\alpha)^2 + 2\alpha(1-\alpha)N(0, z_2) + \alpha^2 N(z_2, z_2)]$ . Figure 3(d) plots  $F(z_2) \equiv \langle(\delta\Phi)^2\rangle / \langle(\delta\theta)^2\rangle$  for several values of  $\alpha$ . For fixed  $R_0$  (with  $R_2 = 1$ ),  $\alpha(k)$  varies periodically from minimum to maximum over the range  $\Delta k = \pi/n_s z_2$ , with then  $\alpha$  determined by the selection of  $k$ .  $F < 1$  represents phase noise reduced below that from thermal fluctuations in the piston phase  $\langle(\delta\theta)^2\rangle$ . Since  $\delta\Phi = 2k[(1-\alpha)\tilde{q}_0 + \alpha\tilde{q}(z_2)]$ ,  $\alpha = 1$  corresponds to direct compensation of the piston phase  $\delta\theta \propto \tilde{q}_0$  for the reflected field, albeit at the price of noise  $\tilde{q}(z_2)$  from fluctuations in the position of the reflecting surface at  $z_2$ . More generally, the minimum  $F_{min}$  for a given value of  $z_2$  represents a compromise in noise from  $\tilde{q}_0$  and  $q(z_2)$  determined by the value  $\alpha_{min}$ .  $F_{min} \simeq 0.36$  for  $z_2 \gg w_0$  and  $\sigma = 0.2$  in Fig. 3(d).

An important caveat related to Fig. 3(d) is that the full curves omit fluctuations in optical path arising from transverse strains  $\epsilon_{xx}, \epsilon_{yy}$ , which contribute by way of  $p_{ij}$  to  $\delta\beta$  and give rise to a scaling  $F \sim z_2/w_0$  for  $z_2/w_0 \gg 1$ . A full treatment of these effects is beyond the scope of our current analysis. Instead, the dashed curve in Fig. 3(d) is from a simple model based upon the FD theorem applied to  $\epsilon_{xx}, \epsilon_{yy}$  with loss angle  $\phi_s$  and provides a rough estimate of their incoherent contribution to  $\delta\beta$ .

The conceptual design in Fig. 3(c) is likely far from optimal. Because the strain field associated with  $\psi(r)$  at  $z = 0$  spreads transversely for  $z > 0$ , it is not well matched to our assumed optical profile with fixed

$w(z) = w_0$ . Geometries with partially reflecting surfaces distributed along  $z$  might further reduce  $F$ . For finite thickness of the substrate, a treatment as in [16] is required, with now the possibility of reflection from the rear surface [27]. More generally, coherent measurements over a range of  $k$  values could enhance sensitivity since  $\delta\beta(k)$  can be tailored to be distinct from  $\delta\theta(k)$ .

Although our treatment has been exclusively for “Brownian” noise arising in the substrate, we suggest that our methods should be relevant to the suppression of thermal fluctuations from other sources within the substrate, such as thermoelastic-damping [16, 18, 19]. Moreover, variations in the coating design from Fig. 2 could lead to schemes for suppression of thermal noise within the coating [23]. In contrast to the substrate for which strains at  $z \ll w_0$  have small correlation with  $\tilde{q}_0$  in the quasistatic regime, thermal noise from the coating leads to surface strains that are highly correlated with  $\tilde{q}_0$ .

Certainly, important questions remain related to our proposals for noise compensation, including significant fabrication challenges, the impact of optical absorption within the coating and substrate, and the need for more complete theoretical analyses. We make no claim of a “magic bullet” for the elimination of thermally driven phase fluctuations in optical interferometry. Rather, our goal is to provide a perspective on thermal fluctuations which moves beyond a surface-centric view to consider the statistical character of the underlying stochastic displacements and strains that conspire to displace the surface and thereby to suggest new strategies for enhanced sensitivity and stability of optical interferometers.

We gratefully acknowledge the guiding hand and critical insights of K. S. Thorne, as well as valuable discussions with V. B. Braginsky, Y. Chen, J. L. Hall, R. Lalezari, and D. R. Nelson. The work of HJK was made possible as a Visiting Fellow at JILA. This research is supported by the NSF and NRC.

Permanent addresses: <sup>†</sup>HJK - Norman Bridge Laboratory of Physics 12-33, California Institute of Technology, Pasadena, CA 91125; <sup>‡</sup>BLL - Department of Physics, University of Illinois, 1110 West Green St., Urbana, IL 61801

- 
- [1] *Systems with Small Dissipation* by V. B. Braginsky and V. P. Mitrofanov (University Of Chicago Press, 1986).
  - [2] K. Numata *et al.*, Phys. Rev. Lett. **91**, 260602 (2003).
  - [3] K. Numata, A. Kemery, and J. Camp, Phys. Rev. Lett. **93**, 250602 (2004).
  - [4] A. D. Ludlow *et al.*, Opt. Lett. **32**, 641 (2007).
  - [5] B. C. Barish and R. Weiss, Phys. Today **52**, 44 (1999).
  - [6] S. Rowan, J. Hough, and D.R.M. Crooks, Phys. Lett. A **347**, 25 (2005).
  - [7] F. Marquardt, A. A. Clerk, and S. M. Girvin, arXiv:0803.1164 [quant-ph] (2008).
  - [8] H. B. Callen and R. F. Greene, Phys. Rev. **86**, 702 (1952).
  - [9] R. F. Greene and H. B. Callen, Phys. Rev. **88**, 1387 (1952).
  - [10] *Statistical Physics* by L. D. Landau and E. M. Lifshitz, Ch. XII (Elsevier, 2006).
  - [11] P. R. Saulson, Phys. Rev. D **42**, 2437 (1990).
  - [12] A. Gillespie and F. Raab, Phys. Rev. D **52**, 577 (1995).
  - [13] N. Nakagawa *et al.*, Rev. Sci. Instrum. **68**, 3553 (1997).
  - [14] Yu. Levin, Phys. Rev. D **57**, 659 (1998).
  - [15] F. Bondu, P. Hello, and J.-Y. Vinet, Phys. Lett. A **246**, 227 (1998).
  - [16] Y. T. Liu and K. S. Thorne, Phys. Rev. D **62**, 122002 (2000).
  - [17] G. M. Harry *et al.*, Cl. Q. Gravity **19**, 897 (2002).
  - [18] V. B. Braginsky, M. L. Gorodetsky, and S. P. Vyatchanin, Phys. Lett. A **264**, 1 (1999).
  - [19] V. B. Braginsky and S. P. Vyatchanin, Phys. Lett. A **312**, 244 (2003).
  - [20] V. B. Braginsky, M. L. Gorodetsky, and S. P. Vyatchanin, Phys. Lett. A **271**, 303 (2000).
  - [21] E. D. Black *et al.*, Phys. Lett. A **328**, 1 (2004).

- [22] E. D. Black, A. Villar, and K. G. Libbrecht, Phys. Rev. Lett. **93**, 241101 (2004).
- [23] G. M. Harry *et al.*, Cl. Q. Gravity **24**, 405 (2007).
- [24] S. D. Penn *et al.*, Phys. Lett. A **352**, 3 (2006).
- [25] M. M. Fejer *et al.*, Phys. Rev. D **70**, 082003 (2004).
- [26] V. B. Braginsky and S. P. Vyatchanin, Phys. Lett. A **324**, 345 (2004).
- [27] F. Ya. Khalili, Phys. Lett. A **334**, 67 (2005).
- [28] *Thin Film Optical Filters* by H. A. Macleod (Taylor & Francis, Inc., Third Edition, 2001).
- [29] Mindlin, Physics **7**, 195 (1936).
- [30] For brevity, henceforth we drop the  $\omega$  subscript for  $\langle \rangle_\omega$ .
- [31] M. Parrinello and A. Rahman, J. Chem. Phys. **76**, 2662 (1982).